Single Crystal Growth and Physical Property Measurements of Sm_3TiX_5 (X = Bi, Sb)

Masahiro Shinozaki[1*], Gaku Motoyama[1] Shijo Nishigori[2] Masahiro Tsubouchi[1] Kiyotaka Miyoshi[1] Kenji Fujiwara[1] and Masahiro Manago[1]

1 Department of Material Science, Shimane University, Shimane 690-8504, Japan
2 ICSR, Shimane University, Shimane 690-8504, Japan
* n20d102@matsu.shimane-u.ac.jp

August 16, 2022

SCES Amsterdam 2022

International Conference on Strongly Correlated Electron Systems (SCES 2022)
Amsterdam, 24-29 July 2022
doi:10.21468/SciPostPhysProc.?

Abstract

We have performed synthesis of single-crystalline samples by flux method and physical properties measurements in Sm_3TiX_5 (X = Bi, Sb). Clear anomalies at T_x around 15 K was observed in both systems. These anomalies at T_x are very sharp and are accompanied by temperature hysteresis. As another feature, the phase transitions at T_x hardly dependent on applying magnetic field at least up to 7 T. Although the detail of the low-temperature phase below T_x is still unclear, it is suggested that these anomalies at T_x are structural transition or valence transition of Sm ions from above behaviors.

Contents

---

1 Introduction

Recently, some compounds with local inversion symmetry breaking have attracted great attention owing to the possibility as a field of odd-parity multipole ordering. The odd-parity multipoles can function as a origin of various unique properties such as cross-correlation phenomena. A zig-zag chain structure lacks a local inversion symmetry and is one of the ideal targets as a candidate of odd-parity multipole ordering [1, 2]. Actually, the magnetoelectric effect originated from magnetic toroidal dipole ordering has been reported on Ce_3TiBi_5 with Ce zig-zag chain structure [3, 4]. The series of compounds represented by R_3TX_5 (R: lanthanoid element, T: transition metal, X: p-block element) has many similar compounds and is expected to be a further research field for odd-parity multipole ordering. Synthesis of these compounds and the investigation of their physical properties are required. We have carried out single crystal growth and physical property measurements of Sm_3TiX_5 (X = Bi, Sb) in which the physical properties are not clear in the present work [5, 6]. On the other hand, recently, it has been reported that some Sm compounds such as $SmOs_4Sb_{12}$ [7, 8] and $SmTi_2Al_{20}$ [9, 10] exhibits the magnetic field insensitive heavy fermion states. Hence, we have also focused on and investigated the behavior of physical properties of Sm_3TiX_5 in a magnetic field.

2 Experimental

Single-crystalline samples of Sm_3TiBi_5 were prepared by a Bi self-flux method. The purities of the materials of Sm, Ti, and Bi are 99.9%, 99.9%, and 99.99%, respectively. The starting materials were placed in the ratio Sm:Ti:Bi = 3:1:50 into a alumina crucible and sealed under high vacuum of 10^{-4} Torr in a quartz tube. The sealed ampoule was heated up 1000 °C, kept for 24 h, followed by a slow cool at 1.2 °C/h to 400 °C. The excess Bi flux was removed from crystals by using a centrifuge. Single-crystalline samples of Sm_3TiSb_5 were prepared by a Sn-flux method. The purities of the materials of Sb and Sn is 99.99% and 99.99%, respectively. The starting materials were weighed in the ratio Sm:Ti:Sb:Sn = 3:1:5:40, and crystals were grown in the same procedure as Sm_3TiBi_5. Obtained single crystals of Sm_3TiSb_5 were etched with 12 M HCl in 30 min in order to remove the residual Sn. The chemical composition determination of samples was carried out by the Energy Dispersive X-ray Spectroscopy (EDS) (Hitachi, Miniscope TM4000Plus). Powder X-ray Diffraction (XRD) was not performed for both systems in this work, because the total amount of obtained crystals was extremely small. Electrical resistivity and specific heat were measured by a standard four-terminal method and a conventional adiabatic heat pulse method. Magnetization measurements were performed using a commercial SQUID magnetometer (Quantum Design, MPMS).

3 Results and discussion

Single crystal specimens of Sm_3TiX_5 (X = Bi, Sb) were successfully grown. The chemical composition ratio of obtained crystals was confirmed as approximately Sm:Ti:X = 3:1:5 by EDS measurements. Maximum size of obtained crystals is $1.5\times(1.0\times1.0)$ mm^3 for Sm_3TiBi_5. However, all obtained single crystal specimens of Sm_3TiSb_5 were very tiny. Typical size and mass of samples of Sm_3TiSb_5 are $0.8\times(0.1\times0.1)$ mm^3 and 0.0002 g, respectively. In order to maintain enough measurement accuracy, only electrical resistivity measurement was performed for Sm_3TiSb_5 in our present work. Additionally, we have also tried single crystal growth of Sm_3TiSb_5 by using other elements as flux: Al, Zn, Ga, In, Pb, and Sb (self-flux). As a result, no single crystals were obtained except for Sn-flux under the preparation condition described in the experimental chapter.

3.1 Sm_3TiBi_5

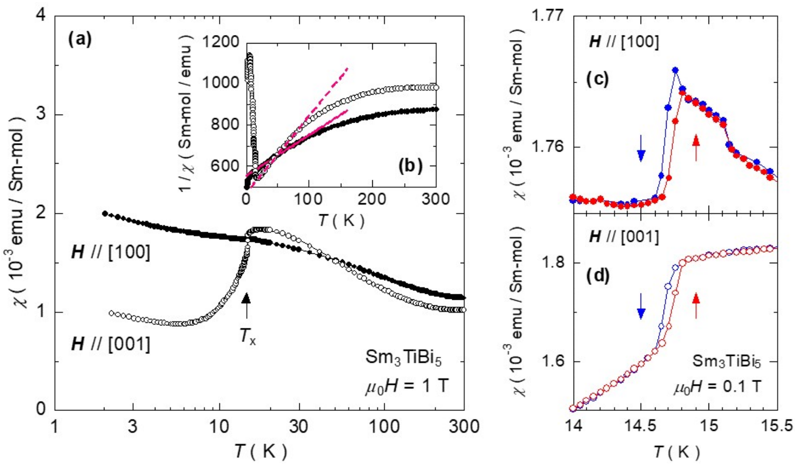

Figure 1: Temperature dependences of **(a)** magnetic susceptibility and **(b)** reciprocal susceptibility of Sm_3TiBi_5 at $\mu_0 H = 1$ T. The solid and dashed lines indicate Curie-Weiss fitting within $T = 30$ K to 80 K in Fig. 1**(b)**. Temperature dependences of magnetic susceptibility of Sm_3TiBi_5 near T_x in the magnetic field direction along **(c)** [100] and **(d)** [001].

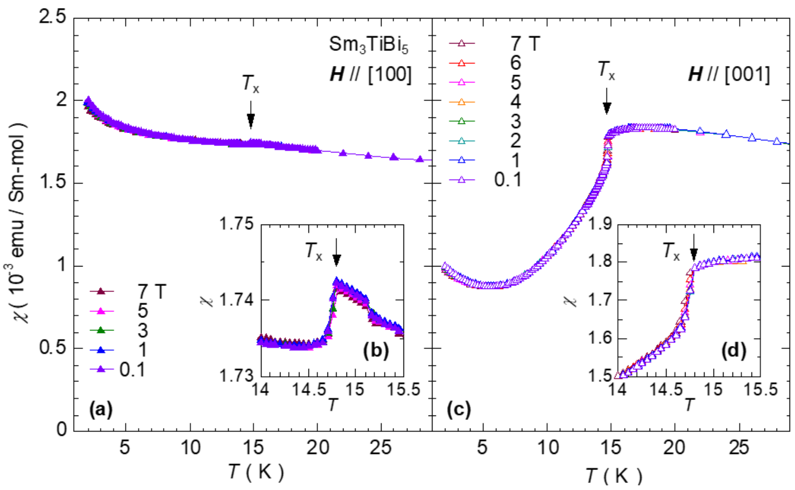

Figure 2: **(a) (b)** Temperature dependences of magnetic susceptibility of Sm_3TiBi_5 below 30 K at applying several magnetic field. **(c) (d)** Inset shows an enlarged view near T_x.

Figure 1(a) shows temperature T dependence of magnetic susceptibility χ of Sm_3TiBi_5 at 1 T. The anisotropy of $\chi(T)$ between $\boldsymbol{H}$ // [100] and [001] is small in the paramagnetic state from $T = 300$ K to around 20 K, and $\chi(T)$ gradually increases with decreasing temperature. The characteristic of $\chi(T)$ on the high T region is that $\chi(T)$ does not follow Curie-Weiss law as shown Fig. 1(b). Temperature dependences of reciprocal magnetic susceptibility in both directions do not follow T-linear dependence over a wide T range. This suggests that the valence of Sm ion changes with temperature change at least in this T range. The effective magnetic moments μ_{eff} and Weiss temperature Θ_p are estimated by the fitting to the Curie-Weiss law within the lower T ranges 30 K to 80 K. The formula $\chi = (T–\Theta_p)/C$ is used for the fitting function, where C is the Curie constant. Obtained μ_{eff} values are 2.01 μ_B and 1.46 μ_B

for the [100] and [001] directions, respectively. The μ_{eff} value in the [001] direction is close to the expected value of free Sm^{3+} ion including the Van Vleck contribution (1.53 μ_B). However, the μ_{eff} value in the [100] direction takes a value between Sm^{3+} and Sm^{2+} (3.40 μ_B). Θ_p are obtained as –280 K and –125 K for the [100] and [001] directions, respectively. This suggests an effective antiferromagnetic (AFM) interaction between the $4f$ electrons. In low T region of Fig. 1(a), a clear anomaly at $T_x = 14.8$ K can be observed. Although gradually increasing of $\chi(T)$ toward $T = 0$ K is common feature, there is a large anisotropy of $\chi(T)$ between $\boldsymbol{H}$ // [100] and [001] below T_x. $\chi(T)$ in $\boldsymbol{H}$ // [100] is almost constant and gradually increases below T_x. In contrast, $\chi(T)$ in $\boldsymbol{H}$ // [001] is after being suddenly suppressed just below T_x, then it also gradually increases. These features below T_x resemble $\chi(T)$ in an AFM ordered state in which the ordered magnetic moments orient in (001) plane. Figure 1(c) and (d) show $\chi(T)$ around T_x. Clear kinks of $\chi(T)$ can be confirmed, and temperature hysteresis behavior is also observed at T_x in both directions. Thus, the anomaly at T_x is considered something first-order phase transition. Figure 2 show $\chi(T)$ under various applied magnetic field condition at low T region. Both the absolute value of χ and T_x hardly change for the magnitude of magnetic field and are seen to maintain almost same value at zero filed. These features indicate a possibility of some ordered state different from the ordinally AFM ordering which is able to be suppressed by the magnetic field. From the constant χ in spite of increasing of magnetic field, the low-T state below T_x is considered to be paramagnetic state. It is considered that the anomaly at T_x is a valence transition of Sm ions or a structural transition, because the phase transition at T_x is non-magnetic first-order transition.

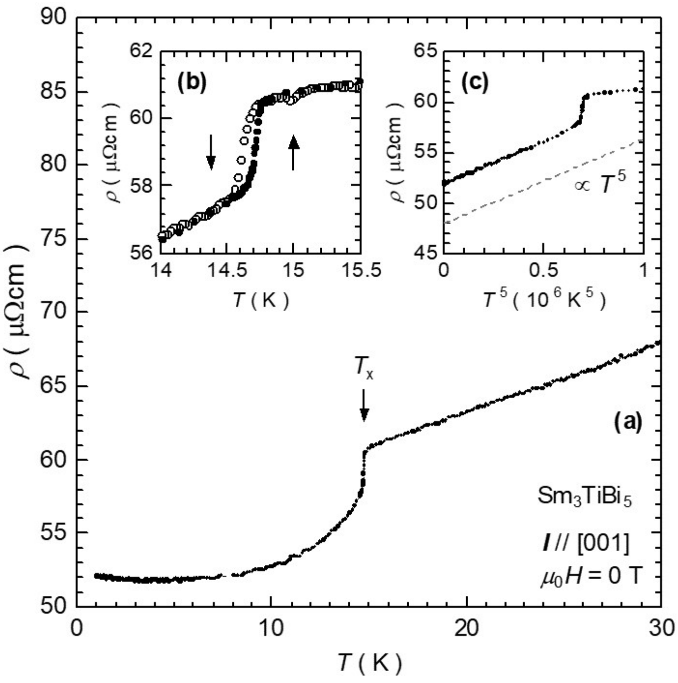

Figure 3: **(a)** Temperature dependence of electrical resistivity of Sm_3TiBi_5 at zero magnetic field. **(b)** An enlarged view near T_x. The solid and open circles are corresponding to heating and cooling, respectively. **(c)** ρ vs T^5 plots below 16 K.

Next, temperature dependence of electrical resistivity ρ of Sm_3TiBi_5 under zero magnetic field condition is shown in Fig. 3. Clear kink of $\rho(T)$ is observed at phase transition temperature $T_x = 14.8$ K which is same temperature estimated by magnetization measurements. $\rho(T)$ rapidly decreases with decreasing T, then becomes almost constant value. This rapidly decreasing of $\rho(T)$ below T_x can be considered due to the decreasing of conduction electron with the valence change of Sm ion from Sm^{3+} or intermediate valence to Sm^{2+}. Temperature hysteresis observed in $\chi(T)$ at T_x also clearly exhibits even in $\rho(T)$ as shown Fig. 3(b). In Fig. 3(c), it is shown that $\rho(T)$ below T_x exhibits T^5 dependence and follows the formula: $\rho(T) = \rho_0 + AT^2 + \beta T^5$, where ρ_0 is residual resistivity, and A is a coefficient of electron-electron interaction. T^5 term is phonon contribution term in the sufficiently lower T range than the Debye temperature Θ_D ($T \ll \Theta_D/2$). Θ_D of Sm_3TiBi_5 is estimated $\Theta_D = 64$ K below T_x from the following specific heat data in $T = 4$ to 12 K. T^5 term is dominant part of $\rho(T)$ in the low-T phase. This result suggests that the electron correlation becomes sufficiently weak below T_x. Additionally, this is consistent with the scenario in which conduction electrons decrease with valence transition of Sm ion, although there is still the possibility that the phase transition at T_x is the structural transition.

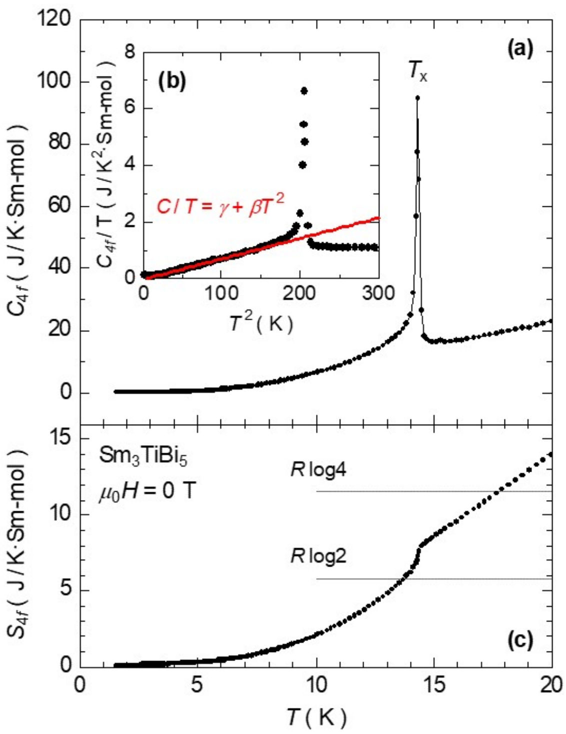

Figure 4: **(a)** Temperature dependence of specific heat of Sm_3TiBi_5 at zero magnetic field. Only the $4f$ electron contribution component is plotted in this graph. **(b)** C_{4f}/T vs T^2 plot of the result of Fig. 4(a). The solid line indicates a T^2 fitting. **(c)** Temperature dependence of magnetic entropy estimated from the result of Fig. 4(a).

Figure 4(a) shows temperature dependence of specific heat C_{4f} of Sm_3TiBi_5 under zero magnetic field condition. C_{4f} is subtracted a lattice contribution by subtracting the specific heat of La_3TiBi_5 from the raw data. A symmetric and very sharp peak was observed at T_x, which is different from a jump of $C(T)$ at second-order phase transition. T_x in Fig. 4(a) is 14.3 K and slightly small value in comparison with that in $\chi(T)$ and $\rho(T)$. From C_{4f}/T vs T^2 curve as shown in Fig. 4(b), the Sommerfeld coefficient γ below T_x is estimated to be almost zero within the measurement accuracy. Curve fitting was performed using the fitting formula: $C/T = \gamma + \beta T^2$, where β is a phonon contribution coefficient. Because γ is very small value, Sm_3TiBi_5 does not considered to be a heavy fermion system and the electron correlation is sufficiently weak below T_x. This is consistent with the above result about the temperature dependence of ρ below T_x. Thus, although the ground state of Sm_3TiBi_5 is hardly dependent phase for magnetic field, it is not field-insensitive heavy fermion state as reported in $SmOs_4Sb_{12}$ and $SmTi_2Al_{20}$. Fig. 4(c) shows the entropy S_{4f} of Sm_3TiBi_5 estimated from the result of C_{4f}.

S_{4f} at T_x reaches about 70% of $R\ln 4$, which indicates that the CEF ground state of Sm_3TiBi_5 is quartet.

3.2 Sm_3TiSb_5

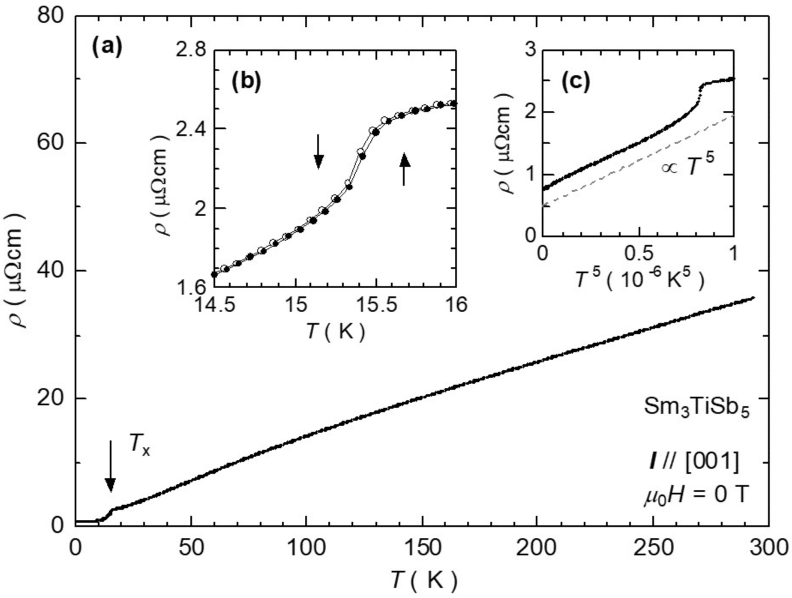

Figure 5: **(a)** Temperature dependence of electrical resistivity of Sm_3TiSb_5 at zero magnetic field. **(b)** An enlarged view near T_x. The solid and open circles are corresponding to heating and cooling, respectively. **(c)** ρ vs T^5 plots below 16 K.

Figure 5(a) shows temperature dependence of electrical resistivity of Sm_3TiSb_5 at zero magnetic field condition. In the high temperature region above 20 K, there are no anomaly and $\rho(T)$ curve shows a T-linear like dependence with slightly upwardly convex. This slight curvature of $\rho(T)$ is considered to be due to the change of the valence of Sm ion with temperature change, similar to that suggested in magnetic susceptibility of Sm_3TiBi_5. $\rho(T)$ exhibits a clear kink at $T_x = 15.5$ K, then $\rho(T)$ only decreases with decreasing temperature. $\rho(T)$ saturates near 5 K and has a constant value at lower temperature. The superconducting transition of residual Sn, which is often seen in RE_3TiSb_5 (*RE*: lanthanoid element) systems grown by Sn-flux method [6, 11], is not confirmed. Hence, our samples seem to be a high purity single crystal with no residual Sn. The residual resistivity ρ_0 at 5 K is 0.76 $\mu\Omega$ cm, and the residual resistivity ratio *RRR* ($= \rho_{300K}/\rho_{5K}$) is about 48. The absolute value of $\rho(T)$ is very smaller than that of previous research, and the *RRR* is about 6 times larger. These features also guarantee our sample quality. A small temperature hysteresis emerges on $\rho(T)$ at T_x as shown in Fig. 5(b). Although the temperature hysteresis of $\rho(T)$ of Sm_3TiSb_5 is smaller than that of Sm_3TiBi_5, as in the case of Sm_3TiBi_5, these clear kink and temperature hysteresis are suggested that the anomaly at T_x is something first-order phase transition. $\rho(T)$ below T_x seems to follow the T^5 dependence as shown Fig. 5(c) similar to the case of Sm_3TiBi_5. Finally, the magnetic field dependence of $\rho(T)$ of Sm_3TiSb_5 is shown in Fig. 6. It can be seen that $\rho(T)$ almost overlaps one another between zero magnetic field and 9 T in both directions of $\boldsymbol{H}$ // [100] and [001]. Although there is a little magnetic resistance, T_x are not change from $T_x = 15.5$ K over the all magnetic field range. These indicate that the phase transition at T_x and the low-temperature phase below T_x in Sm_3TiSb_5 are robust to the external magnetic field just like those of Sm_3TiBi_5.

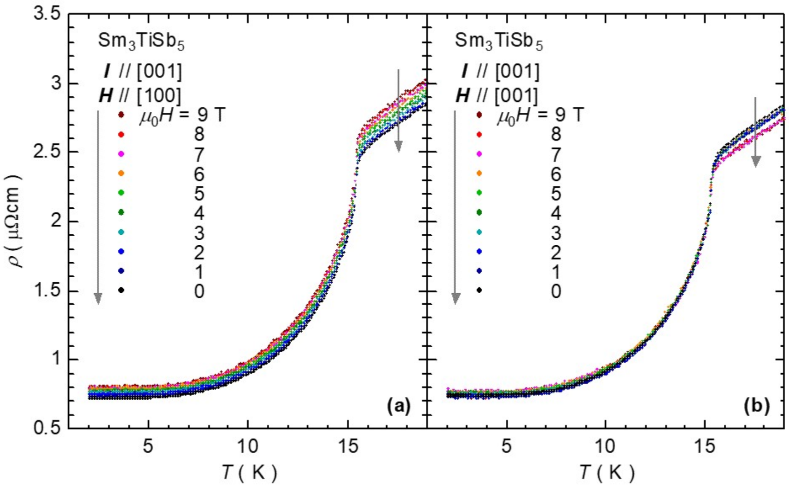

Figure 6: Temperature dependences of electrical resistivity of Sm_3TiSb_5 at applying several magnetic field up to 9 T along the direction **(a)** [100] and **(b)** [001].

4 Conclusion

We have carried out single crystal growth and physical property measurements of Sm_3TiX_5 (X = Bi, Sb). Clear kink at T_x around 15 K was successfully observed in both compounds. Since these kinks at T_x are very sharp and show the temperature hysteresis, it is suggested that these are something first-order phase transition. However, the detail of the low temperature phase below T_x is still unclear. We have also revealed that T_x is hardly dependent on applied magnetic field at least up to 7 T. Following above features, there is a possibility that the anomalies at T_x in Sm_3TiX_5 is structural transition or valence transition of Sm ions.

Acknowledgements

This work was supported by the technical staff at ICSR, Shimane University. The authors thank T. Matsumoto for experimental help. One of the starting materials of 4N purity Sb was provided by NIHON SEIKO Co., Ltd.

Funding information This work was supported by JSPS KAKENHI Grant No. 21K03447.

References

[1] S. Hayami, M. Yatsushiro, Y. Yanagi, and H. Kusunose, *Classification of atomic-scale multipoles under crystallographic point groups and application to linear response tensors*, Phys. Rev. B **98**, 165110 (2018), doi:10.1103/PhysRevB.98.165110.

[2] Y. Yanase, *Magneto-Electric Effect in Three-Dimensional Coupled Zigzag Chains*, J. Phys. Soc. Jpn. **83**, 014703 (2014), doi:10.7566/JPSJ.83.014703.

[3] M. Shinozaki, G. Motoyama, M. Tsubouchi, M. Sezaki, J. Gouchi, S. Nishigori, T. Mutou, A. Ymaguchi, K. Fujiwara, K. Miyoshi, and Y. Uwatoko, *Magnetoelectric Effect in the An-*

tiferromagnetic Ordered State of Ce_3TiBi_5 with Ce Zig-Zag Chains, J. Phys. Soc. Jpn. **89**, 033703 (2020), doi:10.7566/JPSJ.89.033703.

[4] S. Hayami, and H. Kusunose, *Magnetic Toroidal Moment under Partial Magnetic Order in Hexagonal Zigzag-Chain Compound Ce_3TiBi_5*, http://arxiv.org/abs/2208.01754.

[5] G. Bollore, M. J. Ferguson, R. W. Hushagen, and A. Mar, *New Ternary Rare-Earth Transition-Metal Antimonides RE_3MSb_5 (RE = La, Ce, Pr, Nd, Sm; M = Ti, Zr, Hf, Nb)*, Chem. Mater. **7**, 2229–2231 (1995), doi:.10.1021/cm00060a005.

[6] S. H. D. Moore, L. Deakin, M. J. Ferguson, and A. Mar, *Physical Properties and Bonding in RE_3TiSb_5 (RE = La, Ce, Pr, Nd, Sm)*, Chem. Mater. **14**, 4867–4873 (2002), doi:10.1021/cm020731t.

[7] S. Sanada, Y. Aoki, H. Aoki, A. Tsuchiya, D. Kikuchi, H. Sugawara, and H. Sato, *Exotic Heavy-Fermion State in Filled Skutterudite $SmOs_4Sb_{12}$*, J. Phys. Soc. Jpn. **74**, 246–249 (2005), doi:10.1143/JPSJ.74.246.

[8] W. M. Yuhasz, N. A. Frederick, P. C. Ho, N. P. butch, B. J. Taylor, T. A. Sayles, M. B. Maple, J. B. Betts, A. H. Lacerda, P. Rogl, and G. Giester, *Heavy-fermion behavior, crystalline electric field effects, and weak ferromagnetism in $SmOs_4Sb_{12}$*, Phys. Rev. B **71**, 104402 (2005), doi:10.1103/PhysRevB.71.104402.

[9] A. Sakai, and N. Nakatsuji, *Strong valence fluctuation effects in $SmTr_2Al_{20}$ (Tr = Ti, V, Cr)*, Phys. Rev. B **84**, 201106 (2011), doi:10.1103/PhysRevB.84.201106.

[10] R. Higashinaka, T. Maruyama, A. Nakama, R. Miyazaki, Y. Aoki, and H. Sato, *Unusual Field-Insensitive Phase Transition and Kondo Behavior in $SmTi_2Al_{20}$*, J. Phys. Soc. Jpn. **80**, 093703 (2011), doi:10.1143/JPSJ.80.093703.

[11] M. Matin, R. Kulkarni, A. Thamizhavel, S. K. Dhar, A. Provino, and P. Manfrinetti, *Probing the magnetic ground state of single crystalline Ce_3TiSb_5*, J. Phys.: Condens. Matter **29**, 145601 (2017), doi:10.1088/1361-648X/aa57c0.